

## COB-2023-0138

# A STUDY ON THE APPLICABILITY OF GTAW AS AN ENERGY SOURCE FOR DED AND PBF PROCESSES IN ADDITIVE MANUFACTURING

**Alcindo Fernando Moreira**

**Reginaldo Teixeira Coelho**

Department of Mechanical Engineering, São Carlos School of Engineering, University of São Paulo, Av. Trabalhador São-Carlense, 400 – Parque Arnold Schimidt, São Carlos, 13566-590, Brazil.

alcindo@usp.br

rtcoelho@sc.usp.br

**Fábio Edson Mariani**

Department of Production Engineering, São Carlos School of Engineering, University of São Paulo, Av. Trabalhador São-Carlense, 400 – Parque Arnold Schimidt, São Carlos, 13566-590, Brazil.

mariani.fabio@gmail.com

**Abstract.** Additive Manufacturing (AM) processes are currently gaining visibility due to factors such as the possibility of producing complex parts, reduced production time and minimal material removal, resulting in less waste material. However, the high cost of the devices, dimensional limitations of the parts that these devices are capable of producing, and the low energy efficiency of some of the current processes for metal parts are still some of the obstacles to be overcome. The present work evaluated the use of Gas Tungsten Arc Welding (GTAW) welding processes combined with different metal powder feeding for the production of parts using AM. For that, four experimental devices were developed, two based on the Powder Bed Fusion (PBF) process and two based on the Directed Energy Deposition (DED) process. In this study, metallic powder of AISI H13 steel was deposited on an AISI 1020 steel base in single, overlapping, and side by side tracks for analysis of finishing, geometrical, integrity and mechanical properties (Hardness Vickers) parameters. After selecting the most appropriate device, a deposit was built in ten overlapping layers. Therefore, the application of GTAW as an energy source combined with metallic powder constitutes a promising option for producing components through AM.

**Keywords:** GTAW, metal powder, additive manufacturing, WAAM.

## 1. INTRODUCTION

According to the ASTM 52900, (2015(E)) standard, AM is the process of deposition materials, typically layer by layer, from a dataset to build 3D objects in a different way than used in subtractive manufacturing or conformation processes. The currently available methods for producing parts by AM use materials such as photosensitive resins, polymers, ceramics, metals, or combinations of these (composites), depending on the type of production method used. The feedstock can be presented as a solid (wires and sheets), a liquid, or a powder. This manufacturing methodology began to receive more attention in 1986 with Charles Hull's through development of a process known as Stereolithography (SLS). Since then, AM processes have been constantly studied and improved Ngo et al., (2018). Rasiya et al., (2021) highlighted some methods of producing parts by AM based on the type and shape of the feedstock used. In the case of metallic powders, the following methods were highlighted: Selective Laser Sintering (SLS), ProMetal, Electron Beam Melting (EBM) and Engineered Net Shaping Laser (LENS). Laminated Object Manufacturing (LOM) was highlighted for the use of metals in the form of plates and Cold Metal Transfer (CMT), TopTIG, and Plasma Arc Welding (PAW) were mentioned for wires. PAW belongs to the category of production methods by AM defined as Wire Arc Additive Manufacturing (WAAM). According to Li et al., (2022), WAAM has remarkable characteristics such as low cost and greater energy efficiency when compared to other manufacturing technologies in AM. These researchers found that the cost of using the electric arc as a source of fusion energy for AM processes is about 1/10 of the cost of a laser head and 1/30 of the cost of an electron beam generator. According to Treutler and Wesling, (2021), WAAM is a promising methodology for manufacturing parts by AM that uses the combination of electric arc and metallic wires. WAAM is a collective term applied to all methods of manufacturing metal parts by AM that use metal wires as feedstock and the electric arc energy from welding equipment as a heat source for fusion. Given the potential of WAAM, many researchers, such as Li et al., (2022), have dedicated themselves to the study of this manufacturing methodology in AM. Among the welding processes most used by researchers in AM are Gas Metal Arc Welding (GMAW), Gas Tungsten Arc Welding (GTAW), and PAW, as well as variations or combinations of these such as Tandem GMAW, Double-Electrode GMAW (DE-GMAW), and CMT.

Based on the literature review carried out, it was noted that there were no reports of the existence of a WAAM methodology for the manufacture of parts by AM in which GTAW was combined with the addition of feedstock in the form of metallic powder. Additionally, once developed, this manufacturing methodology could also be applied in surface coating processes, where the mechanical characteristics of the surface must differ from the substrate while providing good adhesion.

Such suggested applications comprise a vast field of employment for this new manufacturing methodology, which needs to be better studied and developed so that its full potential as a disruptive technology in the field of mechanical manufacturing processes can be explored. Therefore, the present work proposes the evaluation of the applicability of using the GTAW process for the fusion of metallic powder with the capacity to manufacture 3D objects. In addition to the development of the AM equipment, the objective is also to investigate that the application of the GTAW welding process for the fusion of metallic powder in a controlled manner has the potential to become a low-cost option for the manufacture of certain types of parts, which must go through subsequent finishing processes to reach the shape and dimensional tolerances required in certain applications for high-value equipment.

## 2. METHODOLOGY

To evaluate the applicability of using the GTAW as a source of fusion energy for AM processes that utilize metallic powder as feedstock, four experimental devices were developed. Devices 1 and 2 are based on the PBF process while Devices 3 and 4 are based on the DED process. All devices consist of the following functional parts: a Travelling Torch System, a GTAW Welding Station, and a Powder Handling System.

The Travelling Torch System comprises the following components: a Manrod model MR 300 lathe, a Carriage unit, and a Structure.

The GTAW Welding Station includes the following components: a Miller model Dynasty 210 welding station, a welding torch, and an Argon cylinder with accessories.

Figure 1 illustrates the components of both the Travelling Torch System and the GTAW Welding Station.

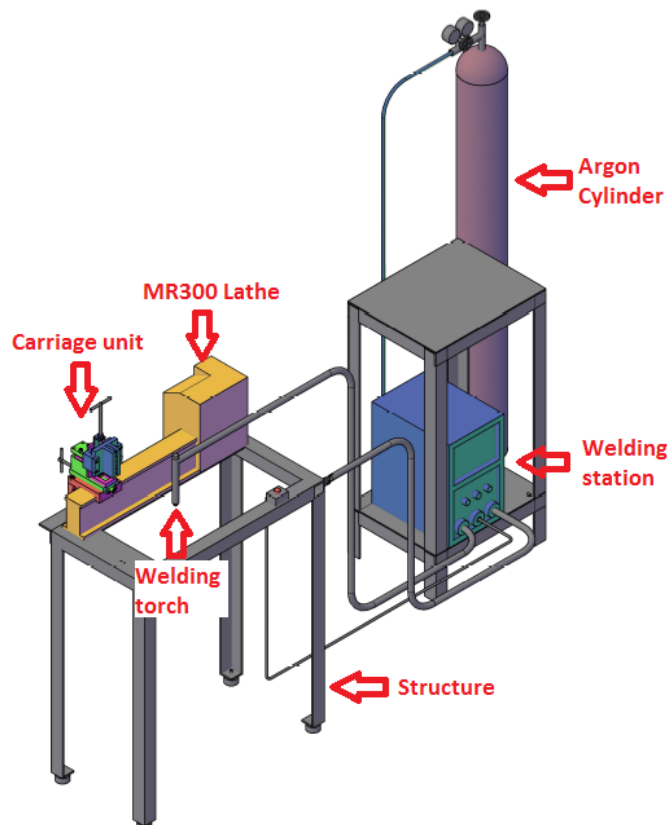
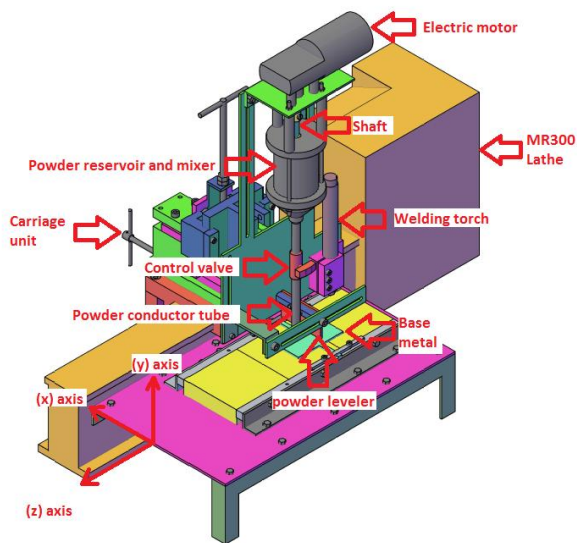
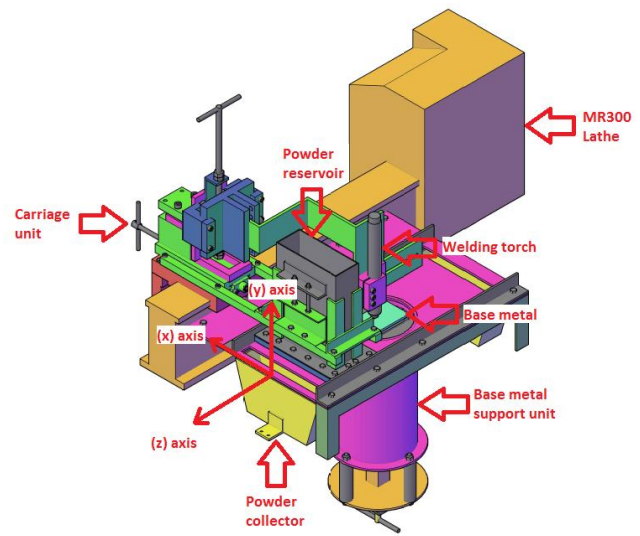


Figure 1 - Travelling Torch System and GTAW welding station components.

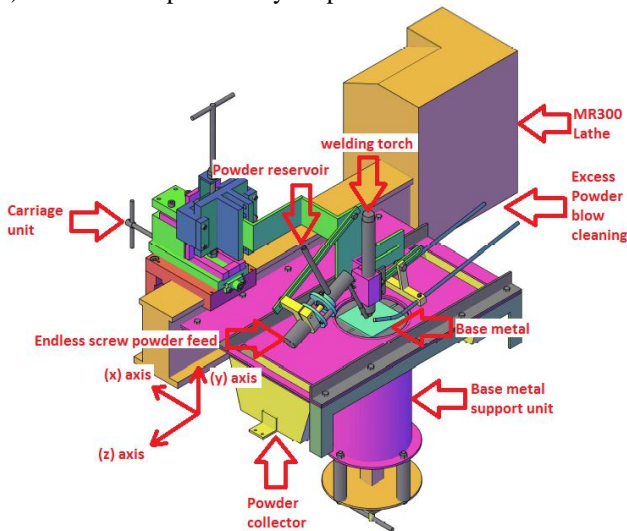
The main difference between the devices lies in the modifications made to the Powder Handling System. Figure 2 a), b), c) and d) highlight the main components of: Device 1 – GTAW with powder layer upon fixed base, Device 2 – GTAW with powder layer upon adjustable base, Device 3 – GTAW endless screw feeder upon adjustable base and Device 4 – GTAW vibrational feeder upon adjustable base, respectively.



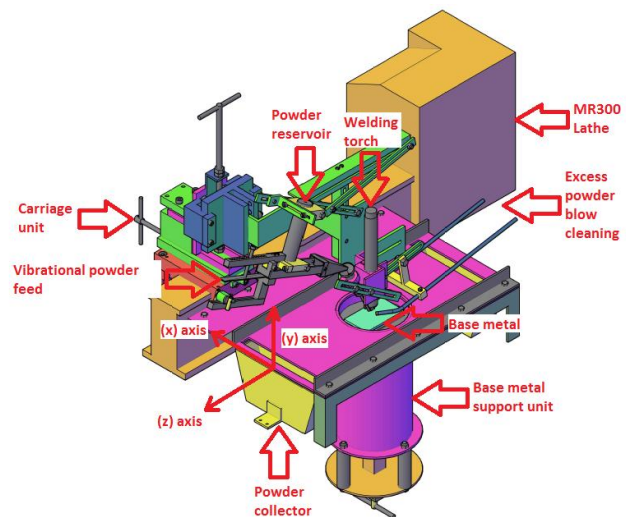
a) GTAW with powder layer upon fixed base



b) GTAW with powder layer upon adjustable base



c) GTAW endless screw feeder upon adjustable base



d) GTAW vibrational feeder upon adjustable base

Figures 2 – a) and b) are based on PBF process and c) and d) are based on DED process.

Powdered AISI H13 steel with a particle size ranging from 53-150  $\mu\text{m}$  was used as the feedstock while AISI 1020 steel plates with a thickness of 3.25 mm served as the base metal. Tungsten electrodes with 2% Thorium (red tip) and diameters of 1.0 mm, 1.6 mm, and 2.4 mm were tested. The welding torch was mounted on a carriage unit adapted from the original carriage of an Manrod model MR300 lathe, enabling automatic torch movement along the (z) axis and manual movement along the (x) and (y) axes.

In Devices 1 and 2, the metallic powder was distributed onto the base metal during movement in the negative direction of the (z) axis. Once the powder distribution was completed, the movement stopped and reversed in the positive direction of the (z) axis. At this stage, the powder was flattened to form layers, followed by the activation of the torch, which melted the powder and allowed it to adhere to the base metal. In Devices 3 and 4, both the feeding and fusion processes occurred in the positive direction of the (z) axis. After completing the deposition of a track, side tracks could be generated along (x) axis by manually operating the handle of the transverse carriage on the carriage unit. This process enabled the generation of new side tracks until the end of the layer.

In Device 1, which featured a fixed base metal support, the welding torch and powder feeding system components (including the electric motor, powder reservoir and mixer, control valve, powder conductor tube, and powder leveler) could be vertically moved upwards along the positive direction of the (y) axis after the end of the layer deposition. This allowed for the deposition of the next upper layer.

In Devices 2, 3, and 4, manipulating the handle of the base metal support unit caused the base metal to move vertically downwards along the negative direction of the (y) axis, allowed the deposition of the next upper layer.

During the deposition process, a comprehensive evaluation of various parameters was conducted to ensure optimal deposition conditions. These parameters include: torch translation speed, welding current, arc length, stick out, cup number, torch inclination, electrode diameter, electrode sharpening, shielding gas flow rate (in Devices 1, 2, 3 and 4); powder layer height (in Devices 1 and 2); powder flow rate, cleaning gas flow rate and positioning of the powder feeder (in Devices 3 and 4). The meticulous examination of these parameters aimed to achieve the best possible deposition outcomes.

The chosen device for AM part production underwent a comprehensive evaluation by conducting single, overlapping, and side by side tracks. This evaluation involved analyzing surface finish, geometric and dimensional data, as well as performing metallographic analyses and Hardness Vickers measurements. The aim was to assess both the physical and metallurgical aspects of the deposits and make necessary corrections to the devices or process based on these observations. Subsequently, a deposit consisting of 10 overlapping layers at 90° angles to each other was produced and thoroughly evaluated, considering the aforementioned parameters. The objective was to draw meaningful conclusions about the applicability of the process in additive manufacturing.

### 3. RESULTS AND DISCUSSION

To evaluate the functionality of Device 1, a total of nine single tracks were initially executed. The process parameters were divided into constant parameters (Table 1) and variable parameters (Table 2).

Table 1 - Constant parameters used for depositing the nine single tracks.

Parameters	Specifications
Base metal material	AISI 1020 steel
Base metal dimensions (length x width x thickness)	100x20x3.25 mm
Feedstock (powder)	AISI H13 steel
Granulometry	53-150 μm
Height of powder layer	1.25 mm
Polarity	CC(-)
Torch inclination	0°
Stick out (distance between cup end and electrode tip)	4.0 mm
Arc length (distance between electrode tip and base metal)	2.75 mm
Argon flow rate	7.0 l/min
Cup number	7
Tungsten electrode diameter	2.4 mm
Tungsten electrode type	2% Thorium
Electrode sharpening angle	37°
Track length	60.0 mm

Table 2 - Variable parameters used for depositing nine single tracks.

Parameter	Values								
	0.625			0.794			0.943		
Torch speed (mm/s)	50	60	70	50	60	70	50	60	70
Current (A)	1	7	4	2	8	5	3	9	6
Base metal number	1	7	4	2	8	5	3	9	6

Figure 3 presents the nine tracks deposited, using Device 1, on AISI 1020 steel plates.

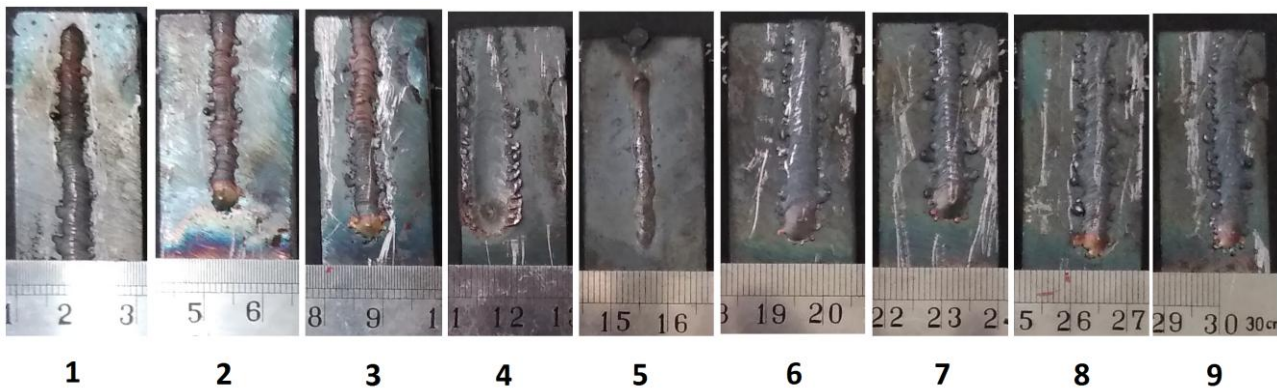


Figure 3 - Single tracks deposited using Device 1

The single tracks were sectioned in the central part to perform measurements related to the width and height of the deposits. These dimensions are presented in Table 3.

Table 3 - Width (W) and height (H) of the nine single tracks using Device 1.

Track	Torch speed (mm/s)	Current (A)	W (mm)	H (mm)
1	0.625	50	4.5	1.5
2	0.794	50	3.5	1.5
3	0.943	50	3.5	1.3
4	0.625	70	6.0	0.5
5	0.794	70	6.0	1.2
6	0.943	70	5.5	1.6
7	0.625	60	4.8	1.6
8	0.794	60	3.8	1.0
9	0.943	60	4.0	1.0

That can be seen after analyzing Table 3 data is that, once the torch displacement speed is fixed, there is a tendency to increase the width of the deposit for higher current values, as observed by Yanhu et al., (2017). In the case of height of tracks, no standard behavior was observed in relation to increases in current. For better analyses of dimensional parameters would be necessary cut the tracks in other points to increase the data sampling and enable a more accurate conclusions. In order to further investigate the deposition process, a deposit labeled as CDPP-01 was generated using the same deposition parameters as track 7, which exhibited the best surface finish in single pass tests. CDPP-01 consists of 10 overlapping passes. Figures 4a), 4b), and 4c) illustrate different stages of the manufacturing process for CDPP-01.

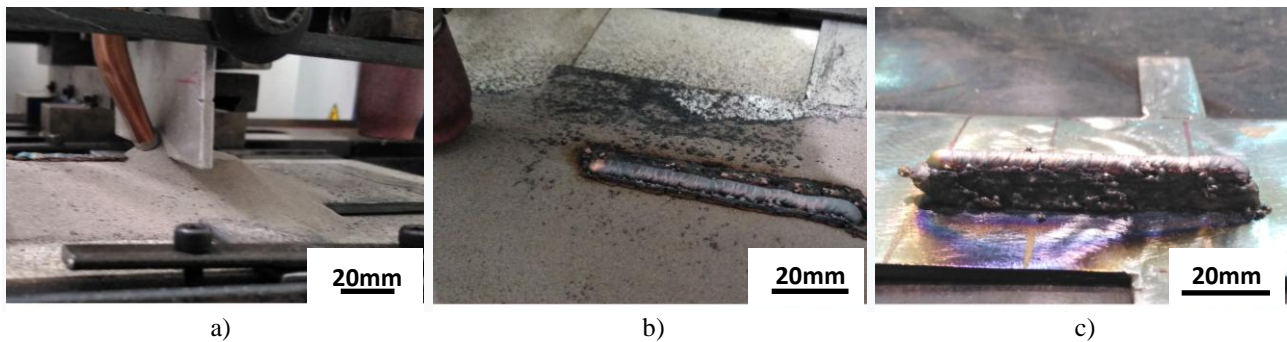


Figure 4 - Phases of CDPP-01 production: a) process initiation, b) deposition completion, and c) post-cleaning.

In order to assess the dimensions of the deposit, measurements of the height (H) and width (W) were obtained at 5.0 mm intervals up to a distance of 30.0 mm from the reference point, using the arc opening point as the reference. These measurements are presented in Table 4.

Table 4 - Height (H) and width (W) measurements obtained at 5.0 mm intervals up to a distance of 30.0 mm from the reference point for CDPP-01.

	Distance from reference point (mm)					
	5	10	15	20	25	30
W (mm)	5.0	5.6	6.0	4.8	4.9	5.2
H (mm)	11.3	11.3	11.3	11.4	11.3	11.0

The width values obtained using Device 1 (4.8 – 6.0 mm) align with the width values reported in the literature (3.5 – 8.0 mm) for WAAM processes that utilize a GTAW source and wire as feedstock (Jhavar et al., 2014 and Matina et al., 2012 *apud* Alberti et al., 2014).

Table 5 presents the Hardness Vickers measurements obtained at 1.0 mm intervals covering the entire height of the wall, from the base metal to approximately 1.0 mm below the top of the deposit. The load applied was 50 gf.

Table 5 - Hardness Vickers values along the centerline of the cross-section of CDPP-01.

Distance from base metal (mm)										
0	1	2	3	4	5	6	7	8	9	10
Hardness Vickers (HV)										
135	131	458	489	423	430	433	545	681	684	679

Additionally, metallographic examinations were conducted on CDPP-01. Figure 5 presents the cross-section of CDPP-01 after etching with 2% Nital.



Figure 5 - Cross-section of CDPP-01 after etching with Nital 2%.

The analysis of Figure 5 reveals a gradual transition in the microstructure. This is an important observation because abrupt changes in microstructure can result in sudden changes in mechanical properties. This finding is further supported by the analysis of the hardness profile, which reveals a decrease in hardness from the highest point of the deposit to the base metal, indicating a thermal influence on the microstructure of the deposited layers, resembling a tempering effect. Additionally, visual examinations did not reveal any pores or cracks.

However, two issues were encountered during the depositions using Device 1. Firstly, there was the presence of small amounts of molten powder that were not completely fused with the melting pool, resulting in balling. This can be observed in Figure 6a. Secondly, there was an instability in maintaining the flatness of the powder layer as the height increased. Figure 6b illustrates this effect.



Figure 6 - a) Incomplete fusion of powder resulting in unattached particles (balling) and b) Instability of the powder layer leading to a “loss of flatness”.

To overcome the challenge of the "loss of flatness" in the powder layer, Device 2, named as GTAW with powder layer upon adjustable base was developed. To evaluate the effectiveness of Device 2 in maintaining the flatness of the powder layer during deposition, a 10-pass overlapping deposition was conducted, resulting in the generation of CDPP-02. Figure 7 presents images of the final layer and post-cleaning stages. The CDPP-02 deposition parameters are contained in Table 6.

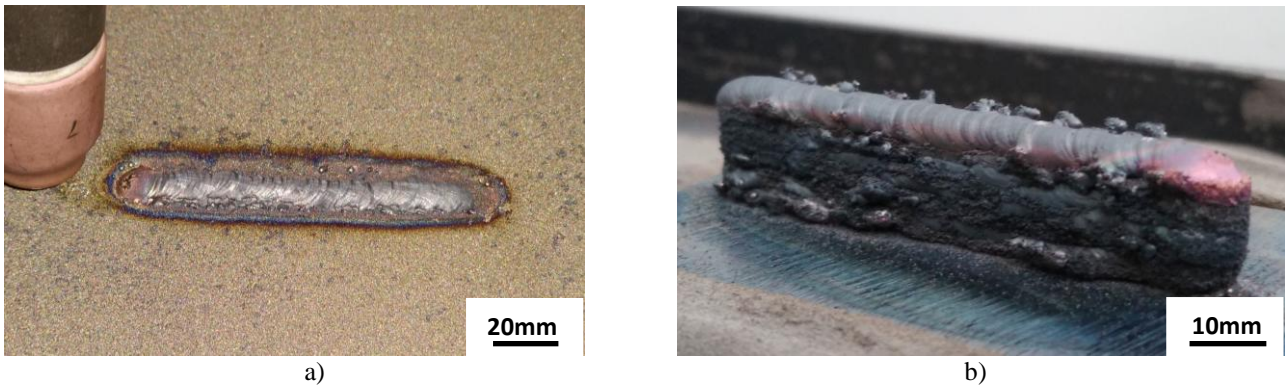


Figure 7 – CDPP-02 deposition stages a) Final layer and b) Post-cleaning.

Table 6 - Deposition parameters for CDPP-02.

Parameters	Specifications
Base metal material	AISI 1020 steel
Base metal dimension (length x width x thickness)	85x50x3.25 mm
Feedstock (powder)	AISI H13 steel
Granulometry	53-150 $\mu\text{m}$
Powder layer height	1.75 mm
Polarity	CC(-)
Current	60 A
Torch speed	0.750 mm/s
Torch inclination	10.5° (clockwise)
Stick out (distance between cup end and electrode tip)	5.0 mm
Arc length (distance between electrode tip and base metal)	2.5 mm
Argon flow rate	7.0 l/min
Cup number	7
Tungsten electrode diameter	2.4 mm
Tungsten electrode type	2% de Thorium
Electrode sharpening angle	37°
Layers number	10

In Figure 7a), it can be observed that the issue of "loss of flatness" of the powder layer has been successfully addressed, resulting in a uniform powder layer around the deposition area. However, the presence of "ballings" on the sides of the track still persisted. These irregularities were believed to be caused by an excess of powder inherent to the PBF process, which in turn led to the deviation of the electric arc too. To overcome this issue, a third device was developed based now on the DED process. This device, named GTAW endless screw feeder upon adjustable base, aimed to mitigate the excess powder related problems. Figure 8 presents single and side by side tracks produced using Device 3, while Table 7 provides the process parameters employed for the depositions.

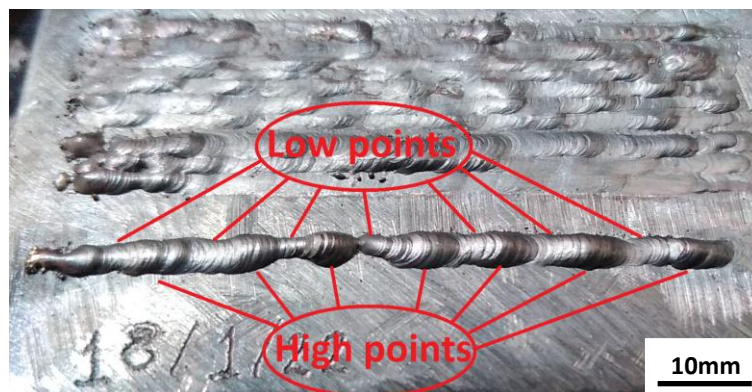


Figure 8 - Single and side by side tracks produced using Device 3.

In Figure 8, it is evident that the issue of "ballings" has been largely resolved. However, the presence of high and low points indicates irregularities in the endless screw powder feeder system. These high points in the tracks also create

challenges in maintaining the direction of the electric arc, necessitating the development of a new powder feeder system, which resulted in Device 4, named GTAW vibrational feeder upon adjustable base.

Table 7 - Parameters used for the deposition of single and side by side tracks using Device 3 shown in Figure 8.

Parameters	Specifications
Base metal material	AISI 1020 steel
Base metal dimension (length x width x thickness)	85x50x3.25 mm
Feedstock (powder)	AISI H13 steel
Granulometry	53-150 $\mu\text{m}$
Polarity	CC(-)
Current	25 A
Torch speed	0,47mm/s
Torch inclination	40° (clockwise)
Stick out (distance between cup end and electrode tip)	10.0 mm
Arc length (distance between electrode tip and base metal)	4.0 mm
Distance from the powder conductor tip to the base metal	6.0 mm
Longitudinal spacing between tungsten electrode and powder conductor tip	2.0 mm
Argon flow rate	7.0 l/min
Powder conductor tube inclination	15° (clockwise)
Cup number	8 (notched)
Tungsten electrode diameter	1.0 mm
Tungsten electrode type	2% Thorium
Electrode sharpening angle	37°
Side-by-side tracks	10
Tracks center line distance	1.5 mm
Excess powder blow cleaning flow rate	6.0 l/min
Powder flow rate	4 RPM

Some tests were performed to evaluate the vibrational feeder system, which showed promising results. The Figure 9 show single, overlapping, and side by side tracks obtained using Device 4.



Figure 9 - Single, overlapping and side by side tracks produced using Device 4.

In Figure 9, corresponding to side by side tracks, is possible observe that in the lower track occurred a arc deviation. Two strategies were thought to try solve this problem: reducing the powder feeding flow rate or increasing the heat input. However, increasing the heat input could result in an undesired increase in track width, which is unfavorable for AM processes. Therefore, the decision was made to decrease the powder feeding flow rate in subsequent tests. Figure

10 shows a top and side view of a deposit (referred as CDPPR-01) consisting of ten layers, consisting ten tracks arranged side by side. The Table 8 provides the process parameters employed for this depositions.

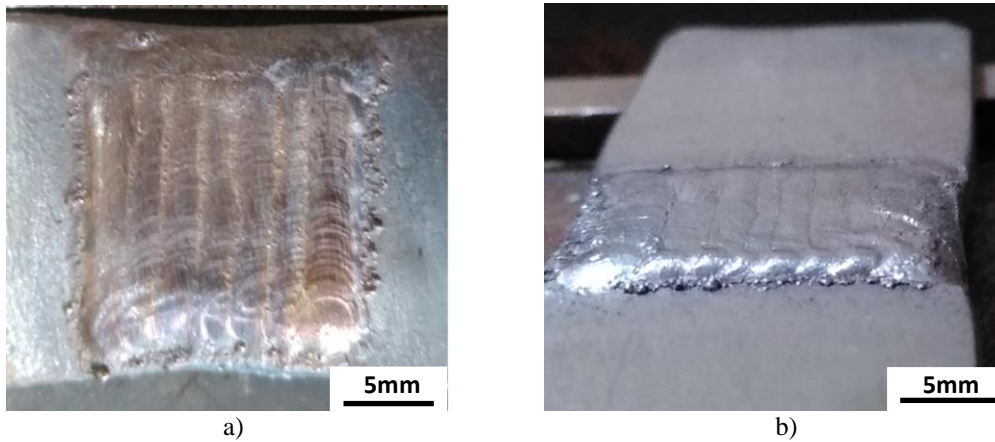


Figure 10 - a) Top and b) side view of CDPPR-01.

Table 8 - Parameters used for the deposition of CDPPR-01.

Parameters	Specifications
Base metal material	AISI 1020 steel
Base metal dimension (length x width x thickness)	85x25.4x3.25 mm
Feedstock (powder)	AISI H13 steel
Granulometry	53-150 $\mu\text{m}$
Polarity	CC(-)
Current	38 A
Torch speed	0.44 mm/s
Torch inclination	18.5° (clockwise)
Stick out (distance between cup end and electrode tip)	10.0 mm
Arc length (distance between electrode tip and base metal)	4.0 mm
Distance from the powder conductor tip to the base metal	5.0 mm
Longitudinal spacing between tungsten electrode and powder conductor tip	4.0 mm
Argon flow rate	4 l/min
Conductor tip inclination	35° (counter clockwise)
Vibrational powder feeding inclination	22° (clockwise)
Cup number	8
Tungsten electrode diameter	1.6 mm
Tungsten electrode type	2% Thorium
Electrode sharpening angle	37°
Tracks center line distance	3 mm
Overlapping between side-by-side tracks	50%
Number of side-by-side tracks	10
Number of layers	10
Excess powder blow cleaning flow rate	6.0 l/min
Powder flow rate	0.5 g/min

Figure 11 shows a cross-section of CDPPR-01. The cross-section of CDPPR-01 deposition exhibited an average hardness of  $200.8 \pm 54.2$  HV. The maximum values obtained for width, height, and penetration were 18.01mm, 0.99mm, and 1.98 mm, respectively.



Figure 11 - Cross sectional view of CDPFR-01. Nital 5% etching.

#### 4. CONCLUSIONS

The application of GTAW as an energy source for AM processes utilizing metallic powder as feedstock is feasible. However, devices based on the PBF process showed lower effectiveness compared to those based on the DED process, mainly due to issues related to arc deviation and balling. The devices based on the DED process require a precise powder feeding system to generate more uniform and repeatable deposits.

Parts produced using GTAW as a fusion energy source and metallic powder as feedstock necessitate subsequent subtractive processes to achieve the final shape and dimensions. In terms of metallurgical aspects, it was observed that the deposit exhibited good adherence to the base metal. Macrographic examinations revealed minimal presence of porosities and cracks and a gradual change in the microstructure was observed from the base metal to the top of the deposit. Problems related to a warping due to excessive heat build-up were observed.

Two factors affect the microstructure and, consequently, the mechanical properties of deposits: dilution and thermal cycles. Deposits that presented higher dilution and were subject to a higher number of thermal cycles, as is the case of CDPFR-01, presented an average Hardness Vickers of 200.8 HV, while deposits that presented lower dilution and were subjected to a smaller number of thermal cycles, as is the case of CDPP-01, presented an average Hardness Vickers of 462.5 HV.

Therefore, the applicability of GTAW as an energy source for AM processes utilizing metallic powder as feedstock has been demonstrated. However, further research and development are needed to make it a cost-effective alternative for additive manufacturing.

#### 5. REFERENCES

- Alberti, E.A., da Silva, L.J., d'Oliveira, A.S.C.M., 2014. Manufatura Aditiva: o papel da soldagem nesta janela de oportunidade. *Soldagem & Inspeção*. Vol. 19. pp. 190-198.
- ISO/ASTM 52900. (2015). Standard terminology for Additive Manufacturing - General principles - Terminology. United States: ISO/ASTM International 2016.
- Jhavar, S., Jain, N.K., Paul, C.P., 2014. Development of micro-plasma transferred arc ( $\mu$ -PTA) wire deposition process for additive layer manufacturing applications. *Journal of Material Processing Technology*. vol. 214. pp. 1102-1110.
- Li, Y., Su, C., Zhu, J., 2022. Comprehensive review of wire arc additive manufacturing: Hardware system, physical process, monitoring, property characterization, application and future prospects. *Results in engineering*. Vol. 13. pp.100330.
- Martina, F., Mehnen, J., Williams, S.W., Colegrove, P., Wang, F., 2012. Investigation of the benefits of plasma deposition for the additive layer manufacture of Ti-6Al-4V. *Journal of Materials Processing technology*. Vol. 212. pp. 1377-1386.
- Ngo, T. D., Kashani, A., Imbalzano, G., Nguyen, K.T.D., Hui, D., 2018. Additive manufacturing (3D printing): A review of materials, methods, applications and challenges. *Composites Part B*, Vol. 143, pp.172-196.
- Rasiya, G., Shukla, A., Saran, K., 2021. Additive Manufacturing-A Review. *Material Today: proceedings*. Vol. 47, pp. 6896-6901.
- Treutler, K., Wesling, V., 2021. The Current State of Research of Wire Arc Additive Manufacturing (WAAM): A Review. *Appl. Sci*. Vol. 11. Pp. 8619.
- Yanhu, W., Chen, X., Konovalov, S.V., 2017. Additive Manufacturing Based on Welding Arc: A low-Cost Method. *Journal of Surface Investigation: X-ray, Synchrotron and Neutron Techniques*. Vol. 11. pp. 1317-1328.

#### 6. RESPONSIBILITY NOTICE

The authors are the only responsible for the printed material included in this paper.